
The Effect of Circuit Structure on Odour Representation in the Antennal Lobe - Mushroom Body Circuit



IISER PUNE

Master's Thesis

Author:

Adithya E Rajagopalan

BS-MS Student

Roll No: 20121018

IISER Pune

Supervisor:

Dr. Collins Assisi

Assistant Professor

Department of Biology

IISER Pune

Certificate

This is to certify that this dissertation entitled "The Effect of Circuit Structure on Odour Representation in the Antennal Lobe - Mushroom Body" towards the partial fulfilment of the BS-MS dual degree programme at the Indian Institute of Science Education and Research, Pune represents original research carried out by Adithya E Rajagopalan at the Indian Institute of Science Education and Research, Pune under the supervision of Dr. Collins Assisi, Assistant Professor, Department of Biology during the academic year 2016-2017.



28/04/17
Adithya E Rajagopalan


28/04/17
Dr. Collins Assisi

Declaration

I hereby declare that the matter embodied in the report entitled "The Effect of Circuit Structure on Odour Representation in the Antennal Lobe - Mushroom Body" are the results of the investigations carried out by me at the Department of Biology, Indian Institute of Science Education and Research, Pune, under the supervision of Dr. Collins Assisi and the same has not been submitted elsewhere for any other degree.


25/04/17
Adithya E Rajagopalan


28/04/17
Dr. Collins Assisi

Acknowledgments

I would like to thank Dr. Collins Assisi for his guidance through the project and for adding theoretical rigour to the project when I lacked it. I would also like to thank all the member of Dr. Assisi's and Dr. Suhita Nadkarni's lab for their advice and help during the course of the project via numerous lab meetings and one on one discussions. My interest in the insect olfactory system and the amazing basis it provides for the understanding of sensory representation and behaviour arose from my summer internships at Janelia Research Campus and I am grateful to Dr. Yoshi Aso and Dr. Gerry Rubin for introducing me to the system. I am thankful to my parents and friends for the support and strength they provided me through this process.

Abstract

Understanding how the structure of neural circuits mediates its function is an area of key interest in neuroscience, particularly in instances where circuits that are trying to accomplish the same over-arching goal, make use of different structural parameters. The antennal lobe - mushroom body circuit of the insect olfactory system - that functions to represent odours experienced by the insect - is one of the most well characterized neural circuits, with physiology and function having been studied in great detail up to the 4th order neurons. In addition there exists significant variations in the structural parameters of this circuit between insects. It therefore provides a useful model in which to understand structure-function relationships. In this thesis I will begin by studying the effect of including temporal structure in neural activity on the function of this circuit. My results suggest that this temporal structure is utilized differently by the circuit depending on the structural parameter regimes adopted, allowing different parameter regimes to function optimally in different conditions. Such results are not predicted by the more simplistic models used in earlier studies, implying that more realistic models of neural circuitry can provide novel insight into its function. I will then show more rigorously that there is more than one regime of structural parameters in which this circuit can perform its function optimally.

Contents

1	Introduction	7
2	Materials and Methods	11
2.1	<i>Model 1 - A snapshot in time</i>	11
2.2	<i>Model 2 - A time-course of activity</i>	12
2.3	<i>Model 3 - Including feedback inhibition</i>	13
2.4	<i>Generating odour representation in projection neuron space</i>	15
2.5	<i>Distance between the representations of two different odours by the same neuronal population</i>	18
3	Results	19
3.1	<i>Maximal input separation does not imply maximal output separation in a snapshot model of the AL-MB circuit</i>	19
3.2	<i>The temporal structure of PN input affects the ability of the KC network to differentiate inputs</i>	20
3.3	<i>Dense connectivity regimes are important to distinguish between inputs that are highly similar</i>	24
3.4	<i>Addition of an autonomous inhibitory feedback loop extinguishes KC spikes and determines sparsity of KC population activity</i>	27
4	Discussions	28
4.1	<i>Size of PN and KC populations explains the lack of correlation between hamming distance and connectivity in the snapshot model</i>	28
4.2	<i>Temporal structure increases dimensionality of inputs allowing different connectivity regimes to differ in function</i>	31

4.3	<i>Glomerular organisation enhances the ability of the MB to distinguish between odours</i>	33
4.4	<i>The difference between the locust and the fly</i>	36
5	Concluding Remarks	37

List of Figures

1	Overview of the insect olfactory system	9
2	Results from the snapshot model of the AL-MB circuit	21
3	Temporal patterning of PN activity affects MB function	23
4	Role of similarity of input on MB function	26
5	Results from the addition of an autonomous inhibitory feedback loop .	29

List of Tables

1	Odours used to test the effect of input similarity on output distance . .	25
2	Sparsity of active KC population with different levels on feedback inhibition	28

1 Introduction

The insect olfactory system is arguably one of the most well characterised neural circuits. Its compactness and simplicity combined with the powerful genetic tools available have allowed for the production of a detailed understanding of its structure and function.

The circuit begins at the olfactory sensory neurons (OSNs) that convert olfactory information from the environment into electrical signals to pass on to the higher brain regions (*Hallem and Carlson 2004a, Hallem and Carlson 2004b, Wilson 2014*). The second level of the circuit is the Antennal Lobe (AL), the principal excitatory neurons in the AL - Projection Neurons (PNs) - represent odours as dense spatiotemporal firing patterns (*Laurent and Davidowitz 1994, Laurent 1996b, Wilson et al. 2004, Wilson 2014*). The structural organisation of the AL varies across species (examples of circuitry in the fly and locust are shown in Figure 1). The AL then feeds information to the Mushroom Body (MB) where sparse firing of the Kenyon Cells (KCs) represent the odour (*Perez-Orive et al. 2002, Turner et al. 2008*). This sparsity is maintained by a high spiking threshold and the inhibitory inputs provided to the KCs by a pair of large GABAergic neurons [Giant GABAergic Neuron - GGN - in locusts, and Anterior Paired Lateral Neurons - APL - in flies] (*Papadopoulou et al. 2011, Masuda-Nakagawa et al. 2014*). These GABAergic neurons are graded neurons whose membrane voltage is mediated by the activity of the KCs, thus forming a feedback inhibition loop [Figure 1]. Synapses immediately downstream of the KCs are plastic and thought to be the primary locus of associative memory in the insect (*Heisenberg 2003*). The KCs pass their information on to the Mushroom Body Output Neurons (MBONs). From the MBONs

onwards neuronal activity is related more with behavioural output than with stimulus representation (Aso et al. 2014, Hige et al 2015).

Such detailed knowledge of the functional roles of each of the neurons involved in the odour processing circuit has begun to be paired with a burgeoning understanding of the connectivity between these cells and the anatomy of the system (*Berck et al 2016*). The structure of the circuitry is important because it is the organization of connections along with the intrinsic properties of the neurons that allow the circuit to perform complex comparisons and computations . Understanding how the structure of networks affects the computations they perform will be integral to figuring out how the circuits perform the functions accredited to them.

These structure-function relationships are of particular interest in instances where circuits that are trying to accomplish the same over-arching goal while making use of different structural parameters. One such instance is the variation in the density of connections between the PNs and KCs across insect species. While the role of the AL-MB circuit is the same across species - ie. to represent odour identity - different species accomplish this goal differently. In the locust, *Schistocerca americana*, every KC receives inputs from approximately 50 percent of all PNs (*Jortner et al. 2007*), whereas in the fly, *Drosophila melanogaster*, every KC receives inputs from only 5 percent of all PNs (*Turner et al 2008*). In addition, the AL of the fly is organized into approximately 50 large glomeruli. Each glomerulus is innervated by the dendrites of 4-10 PNs all of them thus receiving the same inputs [Figure 1]. The locust AL is organized into microglomeruli where every PN receives unique inputs [Figure 1]. In this case ORNs are multi-glomerular unlike in the fly. What do these differences mean for the circuit's ability to represent odours?

It has been shown that the 50 percent PN-KC connectivity seen in the locust max-

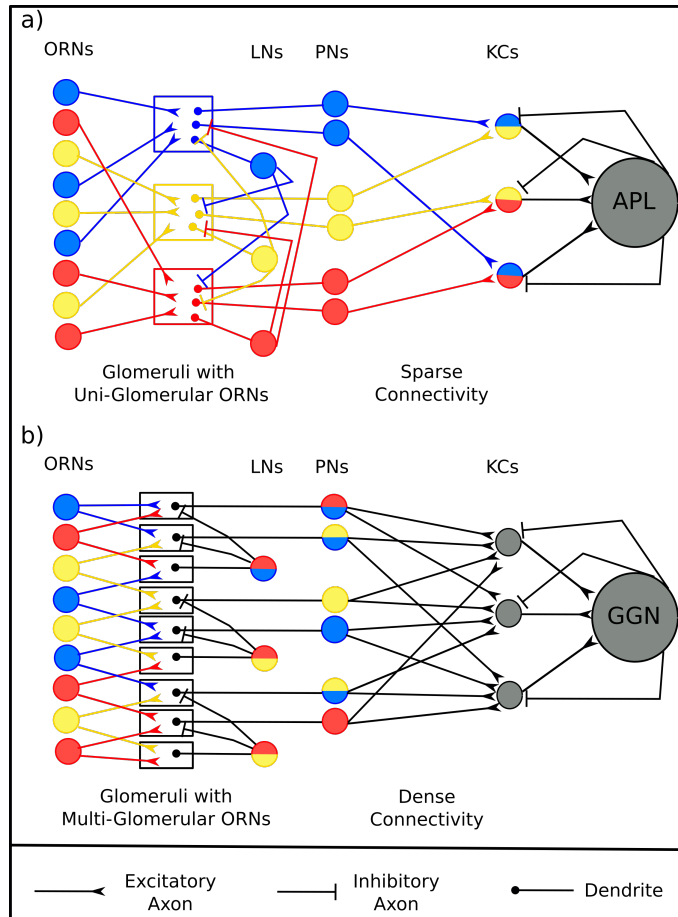


Figure 1: A schematic of the insect olfactory system contrasting the structural parameters of the circuit in *Drosophila melanogaster* (a) and *Schistocerca americana* (b). (a) In the fly all ORNs expressing the same olfactory receptor send their axons to a single glomerulus allowing for the formation of a label-line information coding stream at the level of the AL. LNs (local inhibitory neurons) and PNs receive information from a single one of these glomeruli. LNs that receive inputs from a given glomerulus inhibit PNs and LNs receiving inputs from other glomeruli. PNs transfer this information to the KCs of the MB. In the fly the PN - KC connectivity is sparse - only 5 percent of all PNs synapse onto a given KC. (b) In the locust, ORNs are multi-glomerular, preventing the formation of a label-line code. Also the PN - KC connectivity is dense with approximately 50 percent of all PNs synapsing onto a given KC.

imally differentiates the inputs to the KCs, while the 5 percent connectivity of the fly does this poorly. This is assumed to cause many KCs to have similar activity patterns for several odours (*Jortner 2013*) and would lead to poor odour discrimination. This ability is important for the animals survival. If the locust network was deemed optimal why would a fly, with a circuit designed to solve the same problem, evolve a seemingly sub-optimal configuration. A sub-optimal olfactory network would only make sense if there were other constraints that allowed it to perform its function of representing and distinguishing between odours. My hypothesis is that the glomerular organization of the fly AL does exactly this - it modifies the correlations in the activity of the PNs that is seen by the MB such that a 5 percent connectivity is now sufficient to allow the circuit to represent similar odours differently.

In this study I will begin by building three different models of the PN - KC network. I will use these models to demonstrate that the ability of the KC population to distinctly represent odours that have similar representations in the PN space does in-fact depend upon the extent of connectivity between the PNs and KCs. I will elucidate the role of the temporal structure of PN activity in the KC response and finally show that the glomerular organisation of the fly AL does in-fact perform the function that I hypothesized in the previous paragraph by allowing a network with 5 percent PN-KC connectivity to distinctly represent similar PN population inputs.

2 Materials and Methods

2.1 *Model 1 - A snapshot in time*

The first model used in this study is adapted from the work of Ron Jortner (*Jortner 2013*). It captures a snapshot - a short interval of time - of the activity of the AL-MB circuit [Figure 2a]. In this model the activity of a single PN is denoted by a value of 0 or 1. A value 0 implies that the given PN is inactive, while a value of 1 implies that it is active. The activity of 900 such PNs are strung together to form a 900 element long vector of 1s and 0s that represents the activity of the AL at the time point in consideration [Figure 2a]. These 900 PNs send their outputs to the next layer of cells - the KCs. Each KC receives inputs from a group of PNs. In this study the number of PNs that send their outputs to a single KC varies from 5 to 95 percent of all PNs (in steps of 5 percent). Different odours were simulated by randomly shuffling PN activities. A connectivity matrix is created to map PNs to KCs. The activity of all the PNs that are connected to the same KC were summed to give a value between 0 and the total number of active PNs. It is this summation that the KC sees as its input. To decide which KCs are active, a threshold value is chosen. All KCs that receive an input greater than the threshold are defined as active. The threshold is chosen such that approximately 10 percent of the 50000 KCs in the model are active, as is seen in experimental studies (*Perez-Orive et al. 2002, Turner et al. 2008*).

2.2 Model 2 - A time-course of activity

The second model of the AL - MB circuitry used in this study takes the temporal ordering of neural activity into account [Figure 3a]. Here the activity of a single PN is represented by a 3000 element long vector (with the i th element representing time point i). Each element in this vector can take a value of 1 or 0 - with 1 representing the production of an action potential (AP) by the neuron at that time point and 0 implying the lack of an AP. As in Model 1 the activities of 900 such PNs are strung together to form a 900 X 3000 matrix that represents the activity of the AL in a 3000ms time-course.

Once again, as in Model 1, the PNs were combined to provide inputs to the 50000 KCs, via a connectivity matrix. The KCs were modelled as leaky integrate and fire neurons [eq. 1] (*Turner et al. 2008, Papadopoulou et al. 2011*).

$$C_m * \frac{dV}{dt} = -g_L * (V - E_L) - I_{syn} \quad (1)$$

Here $g_L = 0.089 \text{ mS/cm}^2$, $C_m = 1.0 \text{ } \mu\text{F/cm}^2$ and $E_L = -65.0\text{mV}$. The KC generates a spike when $V > V_{thresh}$. The membrane potential is set to 0mV at the time point of the spike and is reset to -65mV at the next time point immediately after the spike. KCs receive synaptic inputs from the PNs via the term I_{syn} [eq. 1]. These synapses are thought to be cholinergic (*Yasuyama and Salvaterra 1999*) and are modelled as such [eq.2 and 3] (*Destexhe et al 1994, Bazhenov et al. 2001, Perez-Orive et al. 2004, Turner et al. 2008*).

$$I_{syn} = g_{syn} * [O] * (V - E_{syn}) \quad (2)$$

$$\frac{d[O]}{dt} = \alpha * (1 - [O]) * T - \beta * [O] \quad (3)$$

$$T = A * \theta * (t_0 + t_{max} - t) * (t - t_0) \quad (4)$$

In these equations the following terms are constants: $\alpha = 0.94 \text{ ms}^{-1}$, $\beta = 0.18 \text{ ms}^{-1}$, $g_{syn} = 0.05 \text{ mS/cm}^2$, $E_{syn} = 0 \text{ mV}$ and $t_{max} = 0.3 \text{ ms}$. θ is the Heaviside function. $[O]$ is the open probability of the ion channels on the KC membrane and T represents the amount of neurotransmitter released by a given PN. To calculate T at a given time point one needs to know the time elapsed after the most recent PN spike. Once T is calculated, the values for all PNs synapsing onto the same KC are summed and calculation of $[O]$ and I_{syn} follow. These are fed into the calculation of V . This is repeated for each time point in the 3000ms time-course for all 50000 KCs.

2.3 Model 3 - Including feedback inhibition

Another aspect of the AL - MB circuit is the feedback inhibition experienced by the KCs. It is presently assumed that this inhibition happens through a pair of GABAergic neurons (*Papadopoulou et al. 2011, Masuda-Nakagawa et al. 2014*). In the third model used in this study I have included this feedback loop into the circuit [Figure 5a].

Here, PN activity is exactly the same as in Model 2, as is the PN-KC synapse.

There is a slight modification in the equations used to model the KC voltage. In Model 3 KCs receive synaptic input from both the PNs as well as the GGN.

$$C_m * \frac{dV}{dt} = -g_L * (V - E_L) - I_{PN} - I_{GGN} \quad (5)$$

g_L , C_m and E_L are constants with the same value as in Model 2. The equations describing I_{PN} are the same as those for I_{syn} in Model 2, I_{GGN} is the inhibitory current provided to the KC by the GGN. This current is described by the following equations (*Papadopoulou et al. 2011*):

$$I_{GGN} = g_{GGNKC} * S * (V_{GGN} - V_{revGGN}) \quad (6)$$

$$\tau * \frac{dS}{dt} = S_{\infty} - S \quad (7)$$

$$S_{\infty} = \frac{1}{1 + \exp((V_{mid} - V_{KC})/V_{slope})} \quad (8)$$

Here g_{GGNKC} , V_{revGGN} , V_{mid} and V_{slope} are constants. V_{KC} is calculated using eq. 6. This allows you to calculate S_{∞} and S. However to calculate I_{GGN} one also needs the voltage of the GGN. The GGN is modelled as a leaky integrate and fire neuron, similar to the KC model, except that the GGN is a graded neuron (*Papadopoulou et al. 2011*) therefore no spiking condition is required. This is why the calculation of I_{GGN} does not require a knowledge of the most recent GGN spike.

$$C * \frac{dV}{dt} = g_{GGN} * (V_{GGN} - E_{GGN}) - I_{KCGGN} \quad (9)$$

g_{GGN} and E_{GGN} are constants. GGN receives inputs from the KCs via the I_{KCGGN} current. The KC-GGN synapses that give rise to this current are also cholinergic and are described in the same way as the PN-KC synapse (eq. 2, 3 and 4), with the constants modified. Here the constants are α , β , g_{syn} , E_{syn} and t_{max} .

2.4 **Generating odour representation in projection neuron space**

The PN population inputs to the KC network of Model 2 and 3 comprise of a 900 X 3000 matrix of 1s and 0s, with 1s representing a single spike [Figure 3a]. The statistics of the number and timing of the spikes was extracted from the literature. These statistics were then used to generate a population activity of PNs.

PNs fire at a basal rate of 3.87 ± 2.23 spikes per second [eq. 11]; upon odour presentation they generate a spatio-temporal pattern of spikes that continues up to 5 seconds after odour removal (*Perez Orive et al. 2002*). Odour presentation causes an increase in the firing rate of about 10-20 percent of PNs [eq. 10] in the population (*Laurent 1996a, Kee et al. 2015*). These activated neurons fire at a rate of 19.53 ± 10.67 spikes in a 3 second interval starting from odour onset [eq. 12]. Not all PNs show an odour specific response that initiates immediately upon odour onset. Several neurons show increased activity many milli-seconds after odour onset. In addition activity of a single PN appears to be contiguous in time. None of the neurons in the papers that I referenced show increased activity at one

time interval, followed that with a time period of basal activity and then another period of increased activity.

Another important aspect to consider is the presence of oscillations of 20-30Hz frequency (*Laurent 1996b*) in the Local Field Potential (LFP) of the antennal lobe of locust. While not as conclusive, similar oscillations have also been observed in intracellular recordings from *Drosophila* AL (*Tanaka et al. 2009*). The presence of such oscillations suggests that PNs show some correlation during their odour induced activity pattern with more PNs spiking at the peak of the LFP. The oscillations also allow for the division of PN response into smaller epochs of 50ms each (the duration of one oscillation at 20Hz). This division of time into epochs is useful as now one can measure the mean time needed, from start of odour presentation, for an active PN to fire as well as the mean amount of time in which the given PN is active in terms of number of epochs [eq. 13 and 14]

All of the aspects of the odour induced PN population spike pattern mentioned above have been taken into consideration while selecting parameters that would define the PN activity and allow for its artificial generation. The parameters (and their values) used in this process (to simulate 1 second of odour delivery and a 3 second response) are listed below (note all variables are normally distributed and values represent mean \pm standard deviation unless mentioned otherwise) :

$$\text{Percentage of active neurons} = (0.2 \pm 0.05) * (n \text{ of PNs}) \quad (10)$$

$$\text{Basal firing rate} = 3.87 \pm 2.23 \text{ spikes/s} \quad (11)$$

$$\text{Odour induced firing rate} = 19.53 \pm 10.67 \text{ spikes/3s} \quad (12)$$

$$\text{Number of active epochs} = 8 \pm 4 \text{ cycles} \quad (13)$$

$$\text{Number of epochs before activity} = U(1, 20) \text{ cycles} \quad (14)$$

To generate one population PN response, a value of percentage of active neurons drawn from a normal distribution with mean and variance given in eq. 11 is used. This value is used as a probability threshold to decide if a given PN fires or not. For each of the 900 PNs, a uniform random number is drawn to decide if the PN is activated by odour or not. If the random value is less than the probability threshold chosen from eq. 11 then the neuron is odour-activated.

If the neuron is odour-activated then a value of basal firing rate is drawn from eq.12 and spikes equalling three times the value drawn are uniformly and randomly distributed over the 3000 time points. After this a value for odour induced firing rate is drawn from eq.13, number of active epochs from eq.14 and number of epochs before odour-induced activity from eq.15. These three values provide information about which of the LFP oscillation cycles additional spikes needed to be added to the particular neuron's activity as well as how many spikes are to be added in a single epoch. These spikes are then distributed in each of the "active" epochs in such a way that the spike is more likely to occur at the center of the epoch (corresponding to the peak of the LFP) than at the ends.

If the neuron is not odour-activated then only the basal firing rate is defined from eq.12 and the basal spikes are distributed. Once all 900 PNs are described in this way the odour representation is complete.

In the simulations of Models 2 and 3, I have made use of two types of PN input - odours and trials. An odour is defined by the specific PNs that are activated in its corresponding AL representation and parameters drawn from equations 13, 14 and 15 for each of the odour-activated PNs. In different trials of the same odour, the PNs that are activated as well as their parameters remain the same however the exact timing of the spikes in the active epochs change. This timing of spikes as mentioned earlier is drawn randomly (within specified "active" epochs) for each trial. In contrast, two odours differ not only in the timing of spikes of active PNs but also in the identity of the active PNs.

2.5 Distance between the representations of two different odours by the same neuronal population

To quantify the difference in the representation of two different odours by the same neuronal population I made use of a metric called Hamming Distance (HD). The Hamming distance (Figure 2a) compares two vectors of 1s and 0s element-wise and outputs the number of bits that differ between them. This metric was used to define distance between representations both at the AL and the MB level.

The Hamming distance metric was also used in calculating the difference between PN inputs received by any two KCs in the model network [Figure 2b].

3 Results

3.1 *Maximal input separation does not imply maximal output separation in a snapshot model of the AL-MB circuit*

To query the role of PN - KC connectivity in modulating the AL-MB circuit's ability to represent odours, one first needs to ask how different the inputs received by KCs are from one another. This was done by generating a 900 X 50000 connectivity matrix for several values of PN-KC connectivity - ranging from 45 connections per KC to 855 connections per KC (in steps of 45). This matrix was then used to make comparisons between the inputs seen by each possible pair of the 50000 KCs and calculate the mean Hamming distance between them.

The trend seen in the Hamming distances of PN inputs received by any two KCs agrees with earlier results (*Jortner 2013*), with a connectivity of 50 percent maximizing the differences in inputs [Figure 2b]. However, it is the activity of the KCs that represent the odour. If changes in PN-KC connectivity play any role in the function of the circuit then its effect must be noticeable in the KC activity.

To investigate this, I first used a rather simplistic model that has been used in the literature to understand the working of the AL-MB circuit [*Jortner 2013*, *Litwin-Kumar et al 2017*]. This model captures a snapshot of the activity of the circuit [Figure 2a] and has been utilized here to understand how inputs with varying similarity in PN space are differentiated in KC space. Four sets of 101 PN representations, each with a different amount of similarity between any two trials of that set (20, 40, 60 and 80 percent), were fed into this model KC network. The output, population KC activity, was then compared between trial 1 and each of the other trials belonging

to a given set to calculate output hamming distance [Figure 2c].

The ability of the KC population to distinctly represent differing inputs showed no dependence on the amount of connectivity between the PNs and the KCs. While the inputs seen by a given KC are maximally different when PN-KC connectivity is 50 percent, the output distance between KC population representations of two different odours is not maximally different for this value of connectivity. This result agrees with a recent study from *Litwin-Kumar et al. 2017*.

3.2 *The temporal structure of PN input affects the ability of the KC network to differentiate inputs*

An important aspect of the ability of the AL to represent odours that has been neglected in my first set of simulations and in earlier theoretical description of the circuitry [Jortner et al 2007, Jortner 2013, Litwin-Kumar 2017] has been the role of temporal patterning of odour evoked PN activity. To understand the effect that time - and hence a more realistic pattern of inputs - has on the ability of the MB to distinctly represent inputs, I developed Model 2 [Figure 3a].

As an initial test of this model, inputs representing 5 trials of 5 different odours were delivered to the network of integrate and fire KCs. The first set of comparisons I made tested the ability of this description of the network to distinguish between trials of the same odour. I calculated the Hamming distance between the KC population representations of every pair of trials of the same odour and found the mean value for each odour across PN-KC connectivity values. These results [Figure 2b] show that the ability of circuits having sparse levels of PN-KC connectivity is poor when it comes to distinctly representing different trials of the same odour.

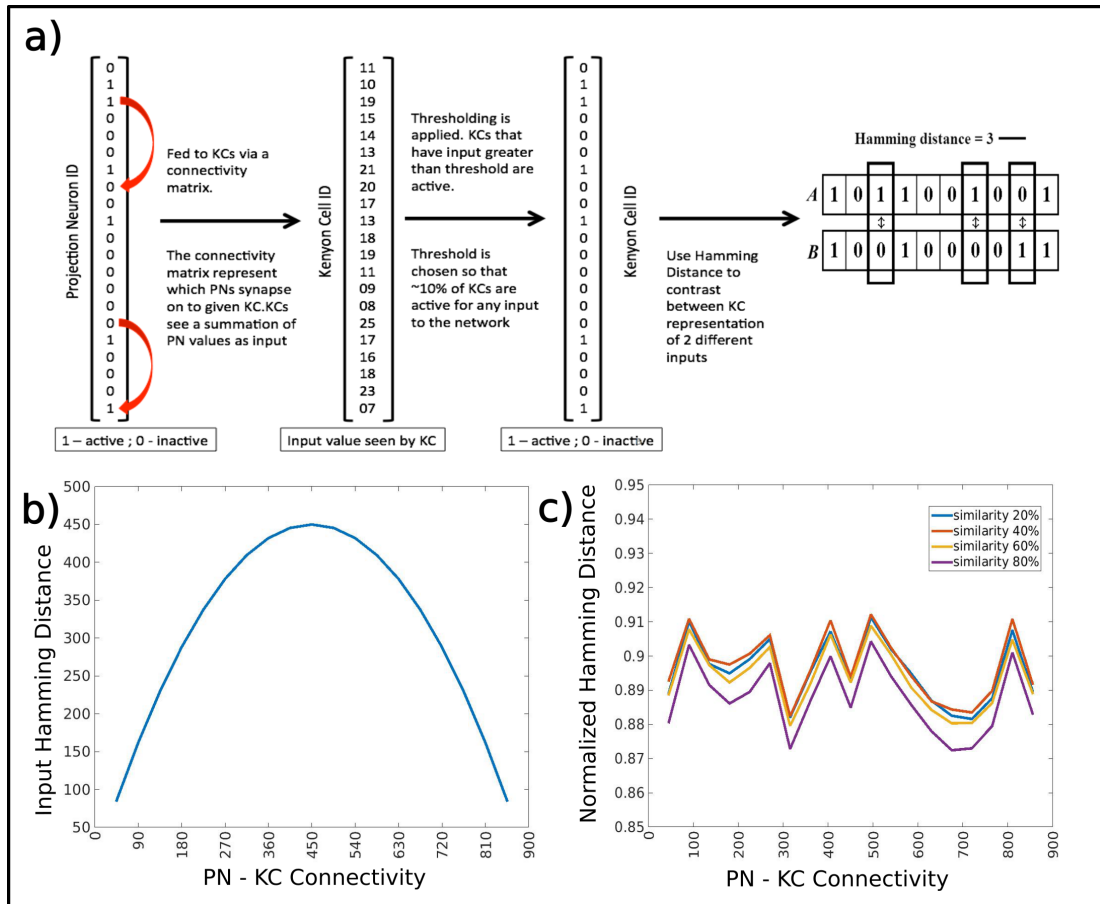


Figure 2: (a) A schematic description of Model 1. The left most vector represents the PN activity. This is permuted through a connectivity matrix to give the input seen by each KC (a 50000 element long vector). Thresholding is then applied to define spiking KCs. PN activity vectors can be shuffled to produce different inputs. The differences between the population representation of two inputs is calculated using a hamming distance measure. (b) The inputs provided to KCs [in all models used in this study] are decided randomly and represented by a connectivity matrix. The hamming distance between inputs seen by two KCs is calculated for all possible pairs and averaged and plotted as a function of the PN-KC connectivity. This graph shows that the distance between inputs is maximized at 50 percent connectivity. (c) The mean hamming distance between the activity of a KC network driven by two different inputs as a function of the PN-KC connectivity value showing that the distance is independent of the PN-KC connectivity.

Whereas circuits having PN-KC connectivity in the 50 - 65 percent range are good at distinguishing between trials. It is important to note here that while the actual values of Hamming distance seen here may not be accurate due to the integration time used in my KC model, the shape of the curve in Figure 2b is likely to remain the same irrespective of the integration time used and it is from this shape that my conclusions are drawn. The integration time I have used is likely to be smaller than that of the actual KC. This small integration time has led the circuit to strongly differentiate between the smallest of changes in the timing of input PN spikes - as can be seen from the HD values in Figure 2b. A more realistic model will reduce the magnitude of the HD while not affecting the shape of the curve.

The next set of comparisons from the data at hand tested the ability of this network to distinguish between odours. I calculated the hamming distance between the KC population representations of every pair of trials of two different odours and found the mean value for each odour across PN-KC connectivity values. These results show that on average the distance between two odours in KC space is high across a large number of connectivity schemes [Figure 3c].

It is to be noted that in my description of the results above, I have neglected the odour representing ability of networks having connectivity denser than 65 percent. This is because as one increases connectivity, the ability of the network to represent odours becomes increasingly variable [Figure 3d and 3e]. In some cases 20 KCs are active in response to trial 1 of an odour while close to 40000 KCs are active in response to trial 2 of the same odour. This variability arises from the similarity of the inputs seen by the KCs in these regimes and the inability to choose a spiking threshold that can consistently allow for the same level of sparsity in the KC population activity. Due to this increased variability, very dense connectivity

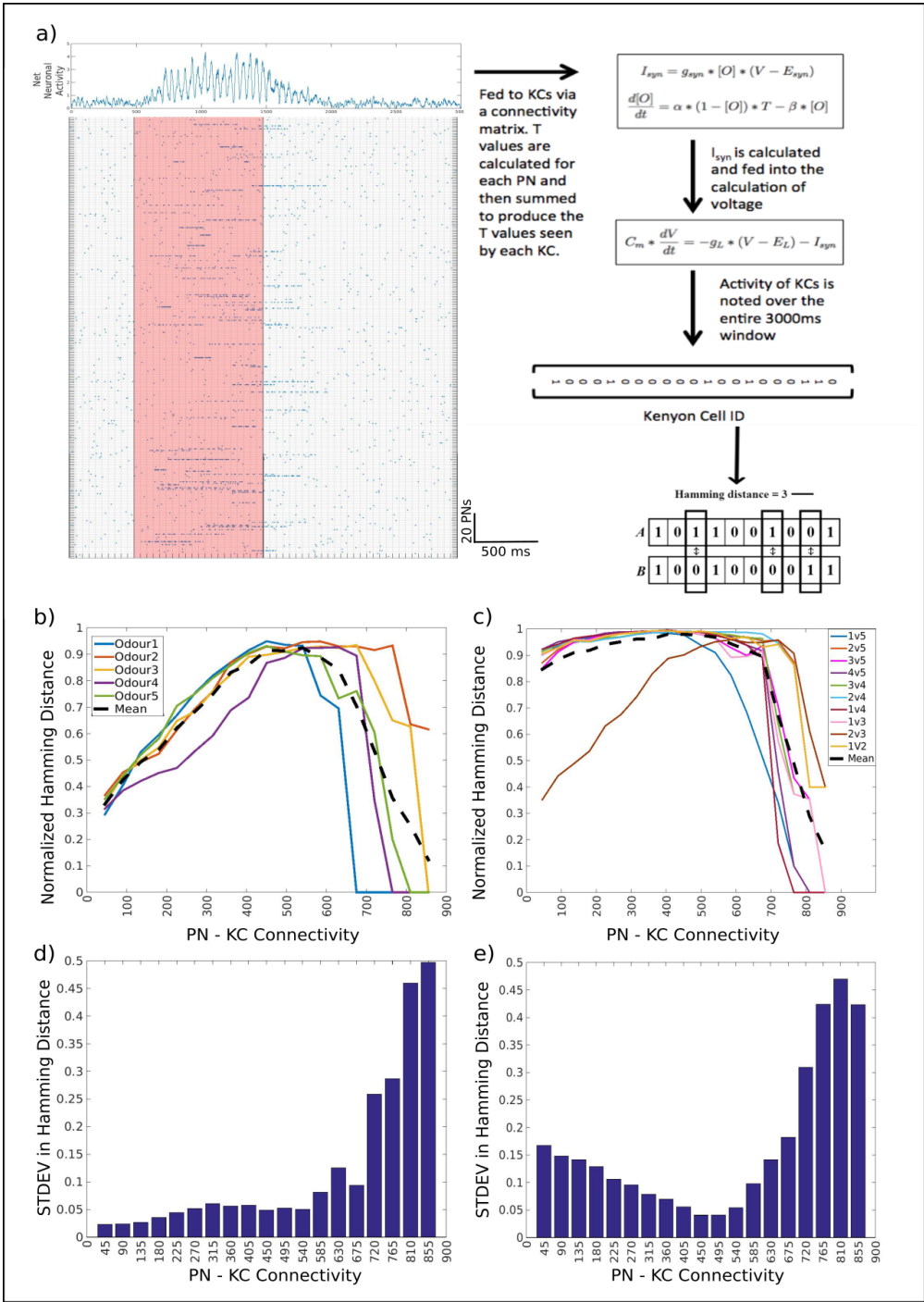


Figure 3

Figure 3: (a) A schematic description of Model 2. The matrix on the left represents the PN activity. These inputs are combined to give the input T values that are used to calculate Isyn. Isyn is fed into the calculation of voltage which is tracked over time to note the activity of KCs. The differences between the population representation of two inputs is calculated using a Hamming distance measure. The mean hamming distance over several trials between the activity of a KC network driven by (b) two different trials of the same odour, and (c) two different odours, as a function of the PN-KC connectivity value. (d) Depicts the mean resolution of the KC network's ability to represent odours as a function of PN-KC connectivity value. (e) Represents the standard deviation in the hamming distance values calculated using different trials of 5 different odours (from (c)). Higher connectivity values show tremendous variation and prove to be unreliable for odour representation.

regimes were not considered in the later simulations.

These results together suggest that the level of similarity of the PN population activity used as inputs plays a role in deciding the network's ability to distinguish between them. While very similar inputs are maximally separated by 50 percent connectivity [Figure 3b] distant inputs can be separated by networks with a range of connectivities from 5 - 65 percent [Figure 3c].

3.3 Dense connectivity regimes are important to distinguish between inputs that are highly similar

To test the effect of the level of similarity of input patterns more systematically, Model 2 was fed with 5 trials of 61 different odour inputs. The 61 odours differed from one another in the PNs that were active. Odours differed by varying amounts as shown in Table 1. The Hamming distances between all trials of odour 1 and all trials of each of the other odours was calculated and pooled again to calculate the mean value for all odour pairs that had the same amount of input difference.

As can be seen from Figure 4, the ability of networks with sparse connectivity to

Table 1: Odours used to test the effect of input similarity on output distance

Odour Number	Amount of Difference from Odour 1
1	Original Odour
2 - 6	5 percent difference in PNs
7 - 11	10 percent difference in PNs
12 - 16	15 percent difference in PNs
17 - 21	20 percent difference in PNs
22 - 26	30 percent difference in PNs
27 - 31	40 percent difference in PNs
32 - 36	50 percent difference in PNs
37 - 41	60 percent difference in PNs
42 - 46	70 percent difference in PNs
47 - 51	80 percent difference in PNs
52 - 56	90 percent difference in PNs
57 - 61	100 percent difference in PNs

distinguish between odours improves with an increase in the difference between inputs. With inputs differing even by only 20 percent the ability of the sparsely connected networks is significantly improved when compared to inputs differing by 5 percent of active PNs. As I will show in my discussion section this improvement, accompanied by the uni-glomerular organisation shown in Figure 1a would improve the ability of sparsely connected circuitry to discriminate between odours. On the other hand, dense connectivity regimes (50 - 65 percent PN - KC connectivity) are successful at discriminating between odours equally well no matter how similar or different they are.

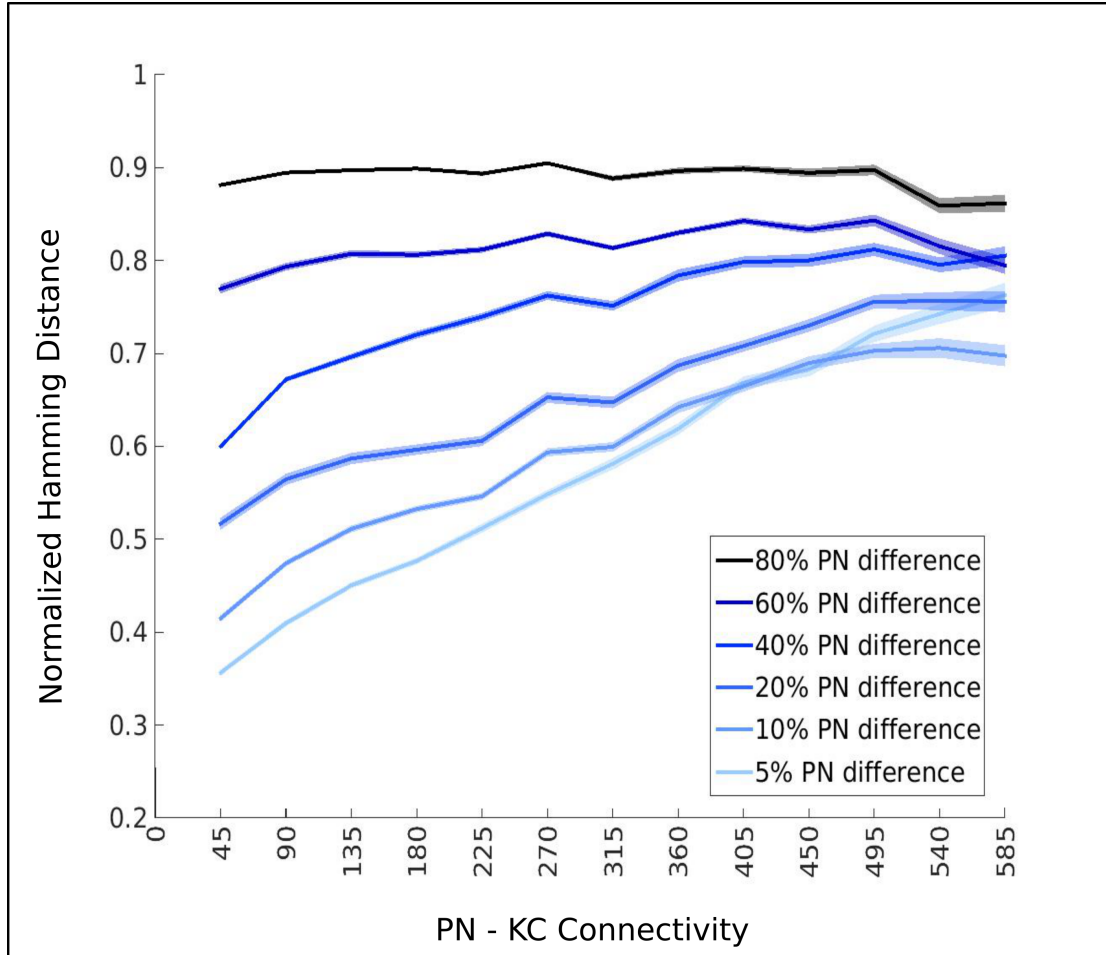


Figure 4: This figure shows the mean Hamming distance (solid line) \pm standard deviation of Hamming distance (translucent area around line) between the activity of a KC network driven by pairs of inputs as a function of PN-KC connectivity. The six lines represent the mean HD between pairs of inputs differing by 5, 10, 20, 40, 60 and 80 percent of all active PNs. The lightest line represents 5 percent PN difference between odours and as the lines get progressively darker the difference between the pairs of odours compared increases. Networks with sparse connectivity are poor at distinguishing between similar odours (5, 10, 20 percent PN difference) but become better at distinguishing between odours as they become more different (40 percent onwards). Dense connectivity networks are effective at distinguishing between all pairs of odours.

3.4 *Addition of an autonomous inhibitory feedback loop extinguishes KC spikes and determines sparsity of KC population activity*

In the simulations depicted so far sparsity of KC population activity was maintained with the help of a voltage threshold that decided when a KC spiked. To ensure that the appropriate sparsity was maintained this voltage threshold needed to be calculated for every odour and for every density of PN-KC connectivity. This was because varying strength of input PN activity affects the voltage of KCs by different extents. While this method performed the desired function it involved a lot of optimisation and was very time consuming.

In the olfactory system this function of spike threshold modification based on the strength of the input is performed through an inhibitory feedback loop. While my artificial modification of spiking threshold was an approximation of this feedback loop, to streamline the simulation process I attempted to implicitly include this feedback loop into Model 3 [Figure 5a]. The following results depict a proof of principle that such a feedback loop can indeed extinguish spikes in the KC and at the population level change sparsity based on the strength of the feedback signal.

The ability of inhibitory feedback to extinguish spikes can be seen in Figure 5b,c. When the same input is provided to a KC without any feedback inhibition as in Figure 5b, this KC spikes 3 times over the time-course of the simulation. Once inhibitory feedback is added two of these spikes are extinguished [Figure 5c]. At a population level, given the same voltage threshold for spiking, different levels of feedback inhibition cause different levels of sparsity in the population KC activity [Table 2]. One measure of strength of inhibition [Table 2] is the conductance of

the KC to the inhibitory current fed to it by the GGN (g_{GGNKC}). While the system works, finding the appropriate parameter values such that the feedback strength changes to ensure same amounts of population activity sparseness for different values of PN-KC connectivity has proven elusive.

Table 2: Sparsity of active KC population with different levels on feedback inhibition with PN-KC connectivity of 5 percent

Model	Number of Active KCs (out of 50000)
no inhibition (ie. $g_{GGNKC} = 0$)	6070
$g_{GGNKC} = 0.2$	1442
$g_{GGNKC} = 0.4$	79

4 Discussions

4.1 *Size of PN and KC populations explains the lack of correlation between hamming distance and connectivity in the snapshot model*

The idea that the PN inputs seen by any two KCs would be maximally different when PN-KC connectivity reached a value of 50 percent (such that a given KC receives inputs from 50 percent of all PNs) arose from a combinatorial argument put forward by *Jortner 2013*. This idea hinges on the fact that the number of ways one can pick i objects from a group of n objects is maximal when $i = \frac{n}{2}$. This implies that when many such combinations of i out of n objects are chosen, the number of differing entities between the objects in each pair of these combinations will be maximal when $i = \frac{n}{2}$. This idea agrees with the data described in Fig. 2b.

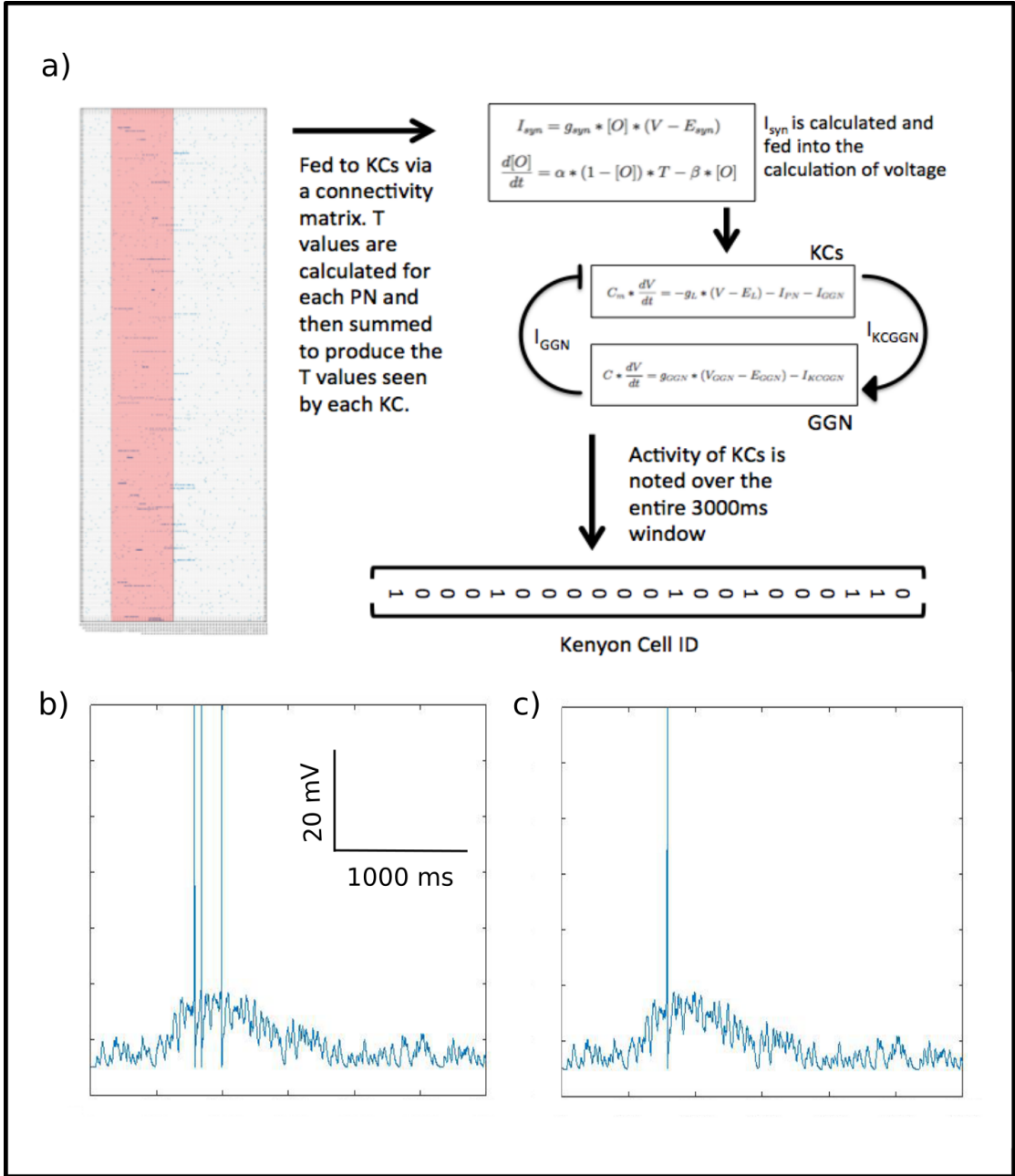


Figure 5

Figure 5: (a) A schematic description of Model 3. The matrix on the left represents the PN activity. This is permuted through a connectivity matrix to give the input T values that are used to calculate I_{PN} . I_{PN} is fed into the calculation of voltage of the KCs. The KC voltage is pooled to provide an input to the GGN which provides feedback inhibition to the KC via GABergic synapses. The voltage of the KCs is tracked over time and their activity is noted. The differences between the population representation of two inputs is calculated using a hamming distance measure. The feedback inhibition provided by the GGN does change the activity of the KC network as can be seen in (b) and (c). (b) represents the activity of a single neuron in a KC network without feedback inhibition. (c) represents the activity of a single neuron in a KC network with inhibition. Inhibition does reduce the spiking activity of cells in the network.

A naive extrapolation of this argument in the context of the KC population activity would suggest that because the inputs to the KCs are maximally different the KC activity would all be maximally different from one another, providing a network with 50 percent connectivity the greatest amount of power to distinguish between inputs. Any difference in the inputs in this regime would lead to a different set of KCs being active. However Figure 2c shows that this is not the case. In fact, there is no dependence between hamming distance and connectivity.

The size of the PN and KC population can explain this unintuitive result. We have a population of 900 PNs. Now consider a 5 percent connectivity regime, in this case 45 out of 900 PNs connect to a given KC. The number of ways in which you can choose 45 out of 900 objects is of the order of magnitude 10^{105} . When you only need to choose 50000 of these combinations there is a very low probability that any two KCs will have the same inputs. Therefore even at a very sparse level of PN-KC connectivity the inputs to the KCs are already more than sufficiently different to allow for KC population activity to distinguish between inputs well.

4.2 Temporal structure increases dimensionality of inputs allowing different connectivity regimes to differ in function

In the case of Model 1, where no temporal patterning of inputs exists, the only criterion that decides whether a particular KC is active or not, is the identity of the PNs that spike. If a sufficient number of PNs (greater than the spiking threshold) connected to a given KC are active in a particular input pattern then that KC will spike. In the case of this model this spiking threshold looks only at the number of active PN inputs, therefore small changes in the identity of the spiking PNs can lead to inputs no longer being greater than threshold and leading to this KC no longer being active. At a population level therefore the group of KCs activated even by similar inputs will be different no matter what the connectivity value. Thus, agreeing with the presented data.

The argument made above however does not hold when temporal structure is added to the inputs provided to the KC network. The activity of PNs has been shown to have a temporal structure that is different and robust for different odours (*Laurent 1996(a); Laurent 1996(b)*). It is the activity of the local inhibitory interneurons that "corrals" these PNs into exhibiting such temporal structure (*Assisi et al. 2011*). This additional level of complexity in odour representation at the level of the AL must be taken into account. When this is done, as in Model 2 and 3, both the identity of the active PNs and the timing of their activity is important in deciding whether KC receives input greater than threshold and spikes. In this situation it is possible for a small number of appropriately timed PN spikes to cause a downstream KC to spike. In essence the temporal structure of inputs adds a dimension to the input seen by the KCs that plays a significant role in deciding whether a KC spikes or not. At low values of PN-KC connectivity, the amount of convergence

of PNs to KCs is low, and hence there is unlikely to be a large enough number of temporally synchronized PNs to cause a KC spike. This implies that the changing just the temporal pattern of inputs will not be sufficient to allow for the KC population to distinctly represent this inputs. This agrees with the data presented in figure 3b and 4. However as the PN-KC connectivity gets denser, the effect of temporal synchrony of PN activity in causing KC spikes will also increase. Therefore any changes in the temporal structure of two inputs will be represented in the KC population activity as seen in figures 3b and 4. As noted earlier, for very dense connectivity values, variability of representation is too high for these regimes to be useful to organisms.

Adding temporal structure to these models therefore allows us to think of the function of sparse and dense connectivity in new ways. It is important to note here that in my analysis of the data produced by Model 2 and 3, I have neglected the temporal structure of the KC activity. While I believe that there is likely to be information stored in the temporal structure of the KC activity, I think that understanding the affect of PN spike timing on the spatial structure of KC activity is of primary importance. Firstly, differences in the temporal structure of PN activity manifests itself as changes in the spatial activity of pattern of the KCs clearly suggesting that this spatial pattern is important. Secondly, the sparsity of KC spikes suggests to me that timing of these spikes is unlikely to carry as much information as there presence or absence alone will. For these reasons I believe that a study of just the spatial activity of KCs provides a useful first picture of how density of PN-KC connectivity affects circuit function.

4.3 *Glomerular organisation enhances the ability of the MB to distinguish between odours*

Including temporal patterning in inputs makes the study of the function of the MB circuitry more realistic. Models of the circuit with different structural parameters now have different functional abilities. An interesting corollary of the results shown so far is that in the sparse connectivity regimes, odours that elicit activity from very similar sets of PNs cannot be distinguished. This would imply that species of insects such as the fly would be poor at distinguishing similar odours. However the uni-glomerular organisation of the PNs seen in the fly could allow the fly to solve this conundrum and enhances the circuit's ability to distinguish between similar odours despite its sparse connectivity.

Consider the following simplistic description of how odours are sensed and processed through the OSNs to give rise to the PN representation in a uni-glomerular insect with 'g' glomeruli. OSNs are represented by a column of 's' vectors with active OSNs getting a value of 1 and inactive OSNs getting a value 0. All OSNs expressing the same Olfactory Receptor (OR) send projections to the same glomeruli. If the vector of OSNs is arranged such that all OSNs expressing the same OR are grouped together, then the following simple matrix multiplication between the OSN vector and 'g' X 's' matrix representing the OSN to glomerulus connectivity, can take you from OSN space to glomerular space.

$$\begin{bmatrix} G_1 \\ G_2 \\ \vdots \\ G_g \end{bmatrix} = \begin{bmatrix} 1 & 1 & 1 & 0 & 0 & 0 & \dots & 0 & 0 & 0 \\ 0 & 0 & 0 & 1 & 1 & 1 & \dots & 0 & 0 & 0 \\ \vdots & \vdots & \vdots & \vdots & \vdots & \vdots & \ddots & \vdots & \vdots & \vdots \\ 0 & 0 & 0 & 0 & 0 & 0 & \dots & 1 & 1 & 1 \end{bmatrix} \begin{bmatrix} OSN_1 \\ OSN_2 \\ \vdots \\ OSN_s \end{bmatrix}$$

A similar matrix multiplication between the vector of activity of glomeruli and the connectivity matrix between PN and glomeruli can give the vector of activity PNs (p elements long).

$$\begin{bmatrix} PN_1 \\ PN_2 \\ PN_3 \\ PN_4 \\ PN_5 \\ PN_6 \\ \vdots \\ PN_p \end{bmatrix} = \begin{bmatrix} 1 & 0 & \dots & 0 \\ 1 & 0 & \dots & 0 \\ 1 & 0 & \dots & 0 \\ 0 & 1 & \dots & 0 \\ 0 & 1 & \dots & 0 \\ 0 & 1 & \dots & 0 \\ \vdots & \vdots & \ddots & \vdots \\ 0 & 0 & \dots & 1 \end{bmatrix} \begin{bmatrix} G_1 \\ G_2 \\ G_3 \\ G_4 \\ G_5 \\ G_6 \\ \vdots \\ G_g \end{bmatrix}$$

Multiplying the two matrices described above will give you a matrix that represents the OSN to PN conversion.

$$\begin{bmatrix} 1 & 1 & 1 & 0 & 0 & 0 & \dots & 0 & 0 & 0 \\ 1 & 1 & 1 & 0 & 0 & 0 & \dots & 0 & 0 & 0 \\ 1 & 1 & 1 & 0 & 0 & 0 & \dots & 0 & 0 & 0 \\ 0 & 0 & 0 & 1 & 1 & 1 & \dots & 0 & 0 & 0 \\ 0 & 0 & 0 & 1 & 1 & 1 & \dots & 0 & 0 & 0 \\ 0 & 0 & 0 & 1 & 1 & 1 & \dots & 0 & 0 & 0 \\ \vdots & \vdots & \vdots & \vdots & \vdots & \vdots & \ddots & \vdots & \vdots & \vdots \\ 0 & 0 & 0 & 0 & 0 & 0 & \dots & 1 & 1 & 1 \\ 0 & 0 & 0 & 0 & 0 & 0 & \dots & 1 & 1 & 1 \\ 0 & 0 & 0 & 0 & 0 & 0 & \dots & 1 & 1 & 1 \end{bmatrix}$$

Each row of this matrix tells you which inputs will be received by a given PN. In such a regime all PNs that receive inputs from the same glomeruli will behave in similar ways in response to odour presentation (as seen from the square blocks of ones which represent PNs that see the same inputs) . There are likely to be more heterogeneities in the actual description of the uni-glomerular- PN olfactory circuit, such as changes in synaptic strength leading to less than perfect correlations in activity between PNs. However, there will still be high correlations between the activities of these PNs (*Dhawale et al. 2010*). This in turn will imply that if any two odours differ by the activity of a single PN they will also differ in the activity of all of its sister PNs. Therefore low levels of difference between inputs is not possible in a uni-glomerular-PN olfactory system model such as the fly.

The clear advantage of this uni-glomerular organization seen in the flies is the ability of this kind of a network to exaggerate the difference between similar odours. Basically if two inputs differ by a single PN in the locust system, they will now differ by an entire glomerulus worth of PNs in the fly. This prevents highly similar odour representations from existing allowing the fly to better discriminate between inputs.

So while the sparse connectivity of the fly is poor at distinguishing between odours that are very similar, when the glomerular organisation of the fly is taken into account one realizes that the PN level difference between such highly similar inputs is exaggerated, allowing the fly to discriminate between them better. Evolution seems to have led to two different solutions, in terms of the parameters of the insect olfactory system, that allow the function of the MB network to be conserved (in terms of odour representation). While the evolution of glomerular organisation may have been driven by other advantages provided by the two configurations,

the configurations that have survived have allowed for different aspect of the MB's function to be maintained at near optimal levels.

4.4 *The difference between the locust and the fly*

These results together suggest that the PN-KC connectivity regimes seen in the locust and the fly are both useful but that they optimize different aspects of KC function. The dense connectivity regimes of the locust are optimal for distinctly representing PN inputs no matter how similar they are whereas the lower connectivity regimes are poor at distinguishing between similar inputs. However the uni-glomerular organization of the fly adjusts PN representations in such a way so as to allow the fly to be a little bit better at odour distinctly representing similar odours than just its low connectivity would allow.

When the only thing that differs between two inputs is the timing of spikes, which in a real life situation is akin to noise, the system still differentiates between inputs when in the locust connectivity regime. This is not useful for the organism. The fly connectivity regime on the other hand does not exaggerate the effect of noise on odour representation which could be crucial in recognizing odours in mixtures and more dynamic environments.

This immediately brings to mind a wide range of experiments that can be performed to test my claims about the ability of the fly and the locust to discriminate between odours. If my claims were true then if one were to teach a fly and a locust to distinguish between two odours, then because of the low effect of noise on odour representation in the fly, it would more quickly learn the difference between the two odours and reach its peak discrimination score. The locust on the other hand

exaggerates noise and inter-trial differences of a given odour. It would therefore take longer to learn which odour was which. However its peak discrimination score is likely to be higher than that of the fly.

5 Concluding Remarks

These simulations express some results that are important not only to the understanding of the function of the olfactory system but also to process of studying such systems in-silico. Temporal patterning of the input to MB affects the ability of this structure to represent and distinguish between odours. Connectivity of the order of 50 percent is the most effective at discriminating between odours. It can separate even very similar odours that differ only by the timing of spikes or by a small number of activated neurons. Sparse connectivity regimes on the other hand are poor at discriminating between similar odours but very good at reducing the effect that noise has on odour representation. Both these characteristics can be useful in their own way depending on the algorithm used by downstream neurons to extract information from these representations. This result agrees with the initial hypothesis put forward by Jortner (*Jortner 2013*), but temporal patterning of neural activity is necessary for this conclusion to be drawn. More simplistic models that do not include a time component suggest that effect of increasing connectivity on improving MB function saturates very quickly (agreeing with Litwin-Kumar et al. 2017). Introducing biological realities into an in-silico model therefore provides an understanding of the function of neural circuitry that cannot be gained from simplistic models.

The introduction of this temporal patterning has also led to the development of

further evidence supporting the idea that a neural circuit can perform its function equally well (while optimizing different aspects of its function) in two different parameter regimes. Such results support the idea that there is no one global optimal solution to a biological problem and that solutions that arise through evolution are ones that work best in the environment in which they have evolved. In this case the environment I am talking about is the environment of other brain structures - such as the AL - and the functions that they perform; but in a broader sense this also includes external environment and organisms with which the our system of interest interacts. Better understanding of the mechanisms underlying circuit function will arise from developing and studying more realistic models for the circuit under study.

References

- [1] Aso, Y., Sitaraman, D., Ichinose, T., Kaun, K.R., Vogt, K., Belliard-guerin, G., Placais, P., Robie, A.A., Yamagata, N., Schnaitmann, C., et al. (2014). Mushroom body output neurons encode valence and guide memory-based action selection in *Drosophila*. *Elife* 1-42.
- [2] Assisi, C., Stopfer, M., and Bazhenov, M. (2011). Using the structure of inhibitory networks to unravel mechanisms of spatiotemporal patterning. *Neuron* 69, 373-386.
- [3] Bazhenov, M., Stopfer, M., Rabinovich, M., Abarbanel, H.D.I., Sejnowski, T.J., and Laurent, G. (2001). Model of cellular and network mechanisms for odor-evoked temporal patterning in the locust antennal lobe. *Neuron* 30, 569-581.
- [4] Berck, M.E., Khandelwal, A., Claus, L., Hernandez-Nunez, L., Si, G., Tabone, C.J., Li, F., Truman, J.W., Fetter, R.D., Louis, M., et al. (2016). The wiring diagram of a glomerular olfactory system. *Elife* 5, 1-21.
- [5] Dhawale, A.K., Hagiwara, A., Bhalla, U.S., Murthy, V.N., and Albeanu, D.F. (2010). Non-redundant odor coding by sister mitral cells revealed by light addressable glomeruli in the mouse. *Nat. Neurosci.* 13, 1404-1412.
- [6] Destexhe, A., Bal, T., McCormick, D.A., and Sejnowski, T.J. (1996). Ionic mechanisms underlying synchronized oscillations and propagating waves in a model of ferret thalamic slices. *J Neurophysiol* 76, 2049-2070.
- [7] Hallem, E.A., and Carlson, J.R. (2004). The odor coding system of *Drosophila*. *Trends Genet.* 20, 453-459.

- [8] Hallem, E. a, Ho, M.G., and Carlson, J.R. (2004). The molecular basis of odor coding in the *Drosophila* antenna. *Cell* 117, 965-979.
- [9] Hige, T., Aso, Y., Modi, M.N., Rubin, G.M., and Turner, G.C. (2015). Heterosynaptic Plasticity Underlies Aversive Olfactory Learning in *Drosophila* Article. *Neuron* 88, 985-998.
- [10] Jortner, R.A., Farivar, S.S., and Laurent, G. (2007). A simple connectivity scheme for sparse coding in an olfactory system. *J. Neurosci.* 27, 1659-1669.
- [11] Jortner, R.A. (2013). Network architecture underlying maximal separation of neuronal representations. *Front. Neuroeng.* 5, 19.
- [12] Kee, T., Sanda, P., Gupta, N., Stopfer, M., and Bazhenov, M. (2015). Feed-Forward versus Feedback Inhibition in a Basic Olfactory Circuit. *PLoS Comput. Biol.* 11, 1-24.
- [13] Laurent, G., and Davidowitz, H. (1994). Encoding of Olfactory Information with Oscillating Neural Assemblies. *Science* . 265, 5-8.
- [14] Laurent, G. (1996). Dynamical representation of odors by oscillating and evolving neural assemblies. *Trends Neurosci.* 19, 489-496.
- [15] Laurent, G. (1996). Temporal Representations of Odors in an Olfactory. *J. Neurosci.* 16, 3837-3847.
- [16] Litwin-Kumar, A., Harris, K.D., Axel, R., and Abbott, L.F. (2017). Optimal degrees of synaptic connectivity. *Neuron* , Volume 93 , Issue 5 , 1153 - 1164.e7
- [17] Masuda-Nakagawa, L.M., Ito, K., Awasaki, T., and O'Kane, C.J. (2014). A single GABAergic neuron mediates feedback of odor-evoked signals in the mushroom body of larval *Drosophila*. *Front. Neural Circuits* 8, 35.

- [18] Papadopoulou, M., Cassenaer, S., Nowotny, T., and Laurent, G. (2011). Normalization for Sparse Encoding of Odors by a Wide-Field Interneuron. *Science* . 721, 721-725.
- [19] Perez-Orive, J., Mazor, O., Turner, G.C., Cassenaer, S., Wilson, R.I., and Laurent, G. (2002). Oscillations and Sparsening of Odor Representations in the Mushroom Body. *Science* . 297, 359-366.
- [20] Perez-Orive, J., Bazhenov, M., and Laurent, G. (2004). Intrinsic and Circuit Properties Favor Coincidence Detection for Decoding Oscillatory Input. *J. Neurosci.* 24, 6037-6047.
- [21] Turner, G.C., Bazhenov, M., and Laurent, G. (2008). Olfactory Representations by *Drosophila* Mushroom Body Neurons. *J Neurophysiol* 99, 734-746.
- [22] Wilson, R.I. (2014). Early Olfactory Processing in *Drosophila*: Mechanisms and Principles. *Annu Rev Neurosci* 217-241.
- [23] Yasuyama, K., and Salvaterra, P.M. (1999). Localization of choline acetyltransferase-expressing neurons in *Drosophila* nervous system. *Microsc. Res. Tech.* 45, 65-79.